Ultrasound-targeted Simvastatin-loaded Microbubble Destruction Promotes OA Cartilage Repair by Modulating Cholesterol Efflux Pathway Mediated by PPARγ in Rabbits.

Xinwei Wang
Nanjing Medical University affiliated Nanjing Hospital: Nanjing First Hospital https://orcid.org/0000-0002-4862-0765

Danbi Wang
Nanjing Medical University

Kai Cheng
Nanjing Medical University affiliated Nanjing Hospital: Nanjing First Hospital

Qi Wang
Nanjing Medical University affiliated Nanjing Hospital: Nanjing First Hospital

Xiaoju Wang
Nanjing Medical University affiliated Nanjing Hospital: Nanjing First Hospital

Qiang Lin
Nanjing Medical University affiliated Nanjing Hospital: Nanjing First Hospital

Jiulong Song
Nanjing First Hospital

Peng Xia
Nanjing Medical University affiliated Nanjing Hospital: Nanjing First Hospital https://orcid.org/0000-0003-3891-3385

Xueping Li (lixueping6504@163.com)
Nanjing Medical University affiliated Nanjing Hospital: Nanjing First Hospital

Research article

Keywords: OA, simvastatin, microbubble, cholesterol efflux, cartilage repair

Posted Date: January 12th, 2021

DOI: https://doi.org/10.21203/rs.3.rs-142167/v1

Abstract

Objective: To evaluate ultrasound-targeted simvastatin-loaded microbubble destruction (UTMD$_{SV}$) attenuation of osteoarthritis (OA) progression in rabbits through modulation of the peroxisome proliferator-activated receptor (PPARγ)-mediated cholesterol efflux pathway.

Methods: In vitro, chondrocytes were treated with ultrasound (US), US-targeted microbubble destruction (UTMD), simvastatin (SV) and UTMD*sv* on alternate days for 4 weeks. Chondrocytes were also treated with PPARγ inhibitor, PPARγ inhibitor+UTMD*sv* and UTMD*sv*. The cholesterol efflux rate and triglyceride were measured respectively by assay kit and oil red O staining. In vivo, the OA rabbits were treated with a single intra-articular injection of UTMD, SV and UTMD$_{SV}$ every 7 days for 4 weeks. Cartilage histopathology was assessed by safranin-O staining and the Mankin score. Total cholesterol (TC) and high-density lipoprotein-cholesterol (HDL-C) in rabbit knee synovial fluid were detected by enzyme-marker assay. Aggrecan, collagen II and PPARγ expression levels were analyzed western blotting (WB).

Results: OA models exhibited primarily by a loss of aggrecan and collagen II, changes to subchondral bone architecture and cartilage degradation. In vitro, UTMD$_{SV}$ significantly increased the cholesterol efflux rate and aggrecan, collagen II and PPARγ levels in OA chondrocytes; these effects were blocked by the PPARγ inhibitor. In vivo, UTMD$_{SV}$ significantly increased aggrecan, collagen II, PPARγ and HDL-C levels, while TC levels and Mankin scores were decreased compared with the UTMD, SV, OA and control groups (95% CI: 0.069 to 6.671).

Conclusion: UTMD$_{SV}$ promotes the expression of aggrecan and collagen II and relieve cartilage degradation by modulating the PPARγ-mediated cholesterol efflux pathway in rabbits.

Introduction

Osteoarthritis (OA) is a clinically chronicand degenerative disease of articular cartilage. The main symptoms of OA are joint pain, stiffness and dysfunction, which are the main causes of physical disability in the elderly[1]. It is generally believed that the pathogenesis of OA is mainly due to the degenerative changes in cartilage caused by chronic joint wear[2]. With advances in epidemiology and molecular biology research related to OA, it is found that the disorder of lipid metabolism plays a key role in the process of OA cartilage degeneration. Therefore, OA has been considered a metabolic disease[3–4].

Cholesterol reverse transport (RCT) represents the process by which excessive cholesterol flows from peripheral cells and combines with high-density lipoprotein (HDL) to form high-density lipoprotein-cholesterol (HDL-C), which is then transported to the liver for metabolic excretion[5]. Several studies have demonstrated cholesterol efflux disorders in OA chondrocytes. This decrease in RCTfunction leads to excessive accumulation of lipids in chondrocytes, leading to hypertrophy and ossification, which exacerbate the degree of cartilage degeneration in OA[6–7]. Peroxisome proliferator-activated receptor γ (PPARγ) play an important role in the mechanism of cholesterol reverse transport regulation, which is a

current research hotspot in the field of lipid metabolism[8]. Some studies have shown that PPARγ knockout rats have severe growth and development defects, and are more likely to suffer from cardiovascular and joint diseases[9–11]. These studies suggested that PPARγ protects against the development of OA in articular cartilage by affecting cholesterol efflux. These studies suggested that PPARγ-mediated cholesterol efflux may be one of the mechanisms that help to promote OA cartilage protection.

Due to poor regeneration of cartilage, the treatment of OA has been a consistent focus of clinical research. At present, commonly used therapeutic drugs for OA, such as non-steroidal anti-inflammatory drugs, can only relieve symptoms and do not attenuate disease progression. Several studies have shown that statins can delay the degeneration of OA chondrocytes by activating PPARγ and promoting cholesterol efflux[12–14]. Therefore, statins are expected to change the course of OA, although long-term oral administration can lead to severe side-effects such as abnormal blood sugar levels, and liver enzyme abnormalities, as well as myopathy, memory and cognitive impairment. Choosing an appropriate route of administration, and shortening the course of treatment to reduce side-effects and enhance the efficacy of statins is a focus of future research.

Ultrasound (US) is a physical factor that can produce mechanicaland cavitation effects, and is widely used in clinical applications. Recently, ultrasound-targeted microbubble destruction (UTMD) has become a promising clinical technology. It involves the delivery of microbubble contrast agents carrying drugs via peripheral veins or local injections followed by the application of US when flowing through the target site. US ruptures the microbubbles to produce a cavitation effect, which increases the cell permeability at the target site, and promotes the rapid release and delivery of drugs, thereby enhancing the therapeutic effect[15]. Currently, research into the application of this technology is focused mainly on the fields of cardiovascular disease and tumor and stem cell therapy[16]. Although a few studies have confirmed that UTMD can be used for the treatment of rheumatoid arthritis[17–18], there are no relevant studies of the application of US-targeted simvastatin-loaded microbubble destruction (UTMD*sv*) for the treatment of OA. In this study, we explored the effect and mechanism of UTMD*sv* on OA cartilage degeneration by modulating the PPARγ-mediated cholesterol efflux pathway.

Methods

OA model establishment in rabbits

This study was approved by the Institutional Ethics Committee of Nanjing First Hospital, Nanjing Medical University (China). All experimental rabbits were provided by Qinglong Shan Animal Breeding Center (China) and were fed standard laboratory food and water and were maintained in a room at the appropriate temperature (25°C, 24 h dark and light cycle). Thirty male New Zealand white rabbits (2.5–3.0 kg) underwent anterior cruciate ligament transection (ACLT) of the right knee[19]. Nine rabbits in the control group underwent a sham operation that did not dissect the anterior cruciate ligament. After

surgery, penicillin (200,000U) was delivered via intramuscular injection twice a day for three consecutive days.

Cell isolation and culture

Four weeks after surgery, rabbits cartilage stemming from OA model group and sham operation group were isolated from the surface of the femoral condyle joint and tibial plateau. The cartilages were minced aseptically and then digested with trypsin and type II collagenase (Gibco, Grand Island, NY, USA). After digestion, chondrocytes were seeded in T25 flasks (5×10^6) in Dulbecco's modified Eagle's medium (DMEM) supplemented with penicillin (50U/mL), 10% fetal bovine serum (FBS) and streptomycin and cultured at 37℃ under 5% CO_2. At 80–90% confluence, the chondrocytes were subcultured in a six-well plate (2×10^6 cells/well) for use in experiments.

immunofluorescence

OA chondrocytes were identified by immunofluorescence staining of aggrecan (MA3-16888, Thermo Fisher, Shanghai, China), collagen II (Origene, MD, USA) and PPARγ (LifeSpan, East Providence, RI, USA) [20]. Chondrocytes were fixed with 4% paraformaldehyde for 10 min, and then blocked with 1% bovine serum (BSA) for 1 h at room temperature. The chondrocytes were labeled for 2 h at 37℃ with antibodies specific for aggrecan, collagen II and PPARγ at 2 μg/ml in 0.1% BSA. Chondrocytes were then incubated with FITC-conjugated secondary antibodies (Agrisera, Vännäs, Sweden; 1:200) for 1 h at 37℃. Nuclei were stained with 4'6-diamidino-2-phenylindole (DAPI, Thermo, Shanghai, China) for 5 min at in the absence of light. Total cells were counted following nuclear DAPI counterstaining in ten random fields per culture dish to determine the number of positive cells.

In vitro $UTMD_{SV}$ intervention experiment

For optimization, the chondrocytes (2×10^6) were treated with US at different intensities (0 W/cm^2, 0.3 W/cm^2, 0.6 W/cm^2, 1.0 W/cm^2) and different concentrations simvastatin-loaded microbubbles (1 μM, 10 μM, and 100 μM). This preliminary experiment showed that 1 μM simvastatin-loaded microbubbles produced the best effect under the parameters of 1 MHz and 0.3 W/cm^2 US irradiation for 30 s. Subsequently, the chondrocytes were treated as follows. (1) Control group - no intervention; (2) US group - US irradiation (1 MHz, 0.3 W/cm^2) for 30 s; (3) UTMD group-naked microbubbles under 1 MHz,0.3 W/cm^2 US for 30 s; (4) SV group – 1 μM simvastatin; (5) $UTMD_{SV}$ group – 1 μM simvastatin-loaded microbubbles under 1 MHz, 0.3 W/cm^2 US for 30 s. All groups were treated once every 2 days for 4 weeks.

PPARγ inhibitor intervention

In the early experiments, we explored the effects of different concentrations of PPARγ inhibitor (T0070907, Selleckchem, Houston TX, USA) on extracellular matrix proteins in chondrocytes. Finally, 12.5 μM T0070907 was selected for use in subsequent experiments[21]. The chondrocytes were seeded in six-well plates (2×10^6 cells/well) and treated as follows. (1) Control group – 0.1% DMSO; (2) PPARγ inhibitor group - treated with 12.5μM T0070907 for 48 h at 37℃; (3) PPARγ inhibitor + $UTMD_{SV}$ group - treated

with 12.5μM T0070907 and 1μM simvastatin-loaded microbubbles under US (1 MHz, 0.3W/cm^2) for 30 s, and continued cultivation for 48 h at 37℃; (4) UTMD$_{SV}$ group - treated with 1 μM simvastatin-loaded microbubbles under US (1 MHz, 0.3W/cm^2) for 30 s and continued cultivation for 48 h at 37℃.

Western blot analysis

Total protein was extracted using lysis buffer (Keygenbio, Nanjing, Jiangsu, China) [4]. After being lysed on ice for 20 min, the lysate was centrifuged (12,000 rpm for 15 min, 4℃) and the supernatant was collected. The protein concentration was analyzed using a bicinchoninic acid protein assay kit (Keygenbio), and the remaining protein was mixed with 5 × sodium-dodecyl sulfate-polyacrylamidegel electrophoresis (SDS-PAGE) buffer and heated at 100 °C for 15 min. Proteins were then separated by SDS-PAGE and electroblotted onto polyvinylidene fluoride (PVDF) membranes. All membranes were blocked with 5% skimmed milk at room temperature for 1 h. Membranes were incubated overnight at 4 °C with the following primary detection antibodies: anti-aggrecan (Thermo Fisher, 1:1,000), anti-collagen II (Origene, 1:1,000), and anti-PPARγ (LifeSpan, 1:1,000). Membranes were subsequently washed three times with Tween-Tris buffered saline (TBST) and incubated with secondary detection antibodies (Keygenbio) at 37 °C for 2 h. After washing as described previously, the proteins were visualized using an enhanced chemiluminescence reagent and quantified using the Image 4000 system (Tanon 6600, Beijing, China). Glyceraldehyde-3-phosphate dehydrogenase (GAPDH, Abcam, Cambridge, USA) was quantified as an endogenous control protein. Quantification of protein expression in WB is relative value, which is the ratio of target protein expression divided by GAPDH (target protein/ GAPDH).

Cholesterol efflux analysis

The cholesterol efflux from chondrocytes was measured using a fluorometric cholesterol efflux assay kit (Sigma–Aldrich, St. Louis, MO, USA)[22]. Briefly, the chondrocytes were seeded in 96-well plates at a density of 2 × 10^4 cells/well and allowed to adhere overnight at 37 °C under 5% CO_2. After adherence, cells were washed with FBS-free Roswell Park Memorial Institute (RPMI, Sigma–Aldrich) medium without FBS. The cells were then labeled with cholesterol and incubated for 16 h at 37 °C under 5% CO_2. Subsequently, chondrocytes were incubated for 5 h (37 °C, 5% CO_2) with 100μL of samples acting as cholesterol acceptors; only FBS-free RPMI was added to the blank control wells. The supernatants (medium) were then transferred to a fresh 96-well plate and the fluorescence was measured (Fm, Ex/Em = 482/515 nm) using a SpectraMax M3 microplate reader (Molecular Devices, San Jose, CA, USA). The adherent cells were solubilized by cell lysis buffer to measure the fluorescence (Fc, Ex/Em = 482/515 nm). The cholesterol efflux (%) was calculated according to the following formula: Cholesterol efflux (%) = Fm/(Fc + Fm) × 100% (Fm = fluorescence intensity of the medium; Fc = fluorescence intensity of the cell lysate).

Oil red O staining

The triglyceride level in chondrocytes was detected using an oil red O staining kit (Keygenbio). The chondrocytes in each group were seeded in a six-well plate (2 × 10^6 cells/well) and incubated for 24 h

(37°C under 5% CO_2). After washing with PBS, the chondrocytes were fixed in 10% neutral formaldehyde for 30 min, and then stained with oil red O staining solution at 60℃ for 10 min. Cells were exposed to decolorizing solutions A and B twice at room temperature. After re-staining with hematoxylin for 20–60 s, the cells were rinsed with decolorizing solution B and observed under a microscope (Olympus BX43, Tokyo, Japan). Isopropanol solution dissolved cells in each group (500 ul/well), and then transferred to a 96-well plate to detect absorbance at 490 nm using a TECAN Infinite M200PRO microplate reader (Thermo).

In vivo intra-articular injection experiment

To optimize the in vivo experiment, we evaluated different ultrasound intensities (1 W/cm^2, 2 W/cm^2) and periods (2 min, 5 min) of intervention in the articular cavity of the right knee of the experimental rabbit. The rupture of simvastatin microbubbles was evaluated using ultrasound images, and the optimal ultrasound parameters (frequency of 1 MHz, intensity of 2 W/cm^2 for 5 min) were identified. The OA model rabbits were randomly divided into four groups using random number table method (n = 6/group) based on the following treatments: OA group, UTMD group, SV group, and UTMD$_{SV}$ group. The sham operation rabbits were used as a control group (n = 6). The treatments were delivered by injection into the right knee joint cavity as follows: UTMD group - naked microbubbles under US irradiation (1 MHz, 2 W/cm^2) for 5 min; SV group – 0.1 mg/mL simvastatin; UTMD$_{SV}$ group – 0.1 mg/mL simvastatin-loaded microbubbles under US irradiation (1 MHz, 2 W/cm^2) for 5 min; control and OA model groups - equivalent volume of saline. Each group received 0.2 mL/kg. All groups were treated once every 7 days for 4 weeks and the rabbits were sacrificed by air embolism for histological and WB analyses after treatment.

T-CHO and HDL-C analysis

Synovial fluid was collected from the knee joint of rabbits and placed at room temperature for 30 min before centrifugation at 4,000r for 5 min. The TC and HDL-C level were determined using oxidase-peroxidase coupling (COD-PAP) test kit (JianCheng bioengineering, Nanjing, China). The absorbance was measured at 510 nm and 546 nm using a TECAN Infinite M200PRO microplate reader (Thermo).

Histological analysis

Histological analysis of articular cartilage was performed for all groups[23]. The femoral condyles and tibial plateau of the right knees were fixed in 10% formaldehyde for 3d. And then were sectioned along the sagittal plane, embedded in paraffin and sectioned after decalcification. Sections were stained with fresh Weigert iron hematoxylin for 5 min, and then washed in running tap water. After soaking for 15 s in acid alcohol differentiation solution (1% hydrochloric acid, 70% alcohol), slides were washed with distilled water for 10 min before immersion in fast green stain for 5 min. Next, the sections were washed briefly with 1% acetic acid for 15 s to remove residual fast green stain. Subsequently, sections were stained with safranin-O for 5 min, dehydrated with 95% alcohol, cleared with xylene and finally sealed in optical resin. The following characteristics of the sections prepared from each group were graded according to Mankin's scoring principles: the tide-line integrity, the number and structure of chondrocytes, and dye

intensity. The severity of tissue lesions was graded and standardized as a scoring criterion, with higher scores reflecting greater severity of the lesion. The sections were evaluated independently by two observers using a blinded method and average scores were calculated as the result.

Statistical analysis

The vivo animal studies were randomized, except for the in vitro cell experiments. No samples or animals were excluded from the analysis except rabbits who died early in the process of experiment (30 rabbits in vivo experiments and 9 rabbits in vitro experiments, no animals were excluded). All in vivo data were expressed as the mean and each data point represents an individual rabbit. All in vitro data are expressed as mean with 95% CI. The data displayed normal variance. The independent *t*-test and one-way analysis of variance (ANOVA) were used to identify the significance of the difference followed by Least significant difference (LSD). All statistical analysis was performed using SPSS software (version 21.0, IBM, USA). $P < 0.05$ were considered to indicate statistical significance.

Results

Cholesterol efflux and extracellular matrix proteins decreases in OA chondrocytes

To test the hypothesis that extracellular matrix (ECM) protein is lost and the disorder of cholesterol metabolism occurs in OA chondrocytes, we established the rabbit OA model by ACLT operation. Western blot analysis confirmed that the expression levels of aggrecan ($P = 0.003$ [CI: 0.27, 0.76]), collagen II ($P = 0.003$ [CI: 0.28, 0.77]) and PPARγ ($P = 0.004$ [CI: 0.38, 0.88]) were significantly reduced in OA group compared with those in the control group [Fig. 1(A-B)]. The cholesterol efflux rate was also decreased ($P = 0.002$ [CI: -30.07, -19.93]) in OA chondrocytes [Fig. 1(C)]. Immunofluorescence analysis of the expression of aggrecan ($P = 0.002$ [CI: -7235, -3185]), collagen II ($P = 0.0003$ [CI: -4737, -2925]) and PPARγ ($P = 0.0004$ [CI: -5781, -3409]) showed that the expression of these proteins as significantly reduced in the OA group compared with the control group [Fig. 1(D-E)].

UTMDsv increases cholesterol efflux and extracellular matrix proteins level in OA chondrocytes

To investigate the effect of UTMDsv on ECM expression and cholesterol metabolic level in OA chondrocytes, we treated OA chondrocytes with US, UTMD, SV and UTMD*sv* respectively. Western blot analysis showed that the expression levels of aggrecan ($P < 0.0001$ [CI: -1.294, -0.755]), collagen II ($P < 0.0001$ [CI: -1.894, -1.075]) and PPARγ ($P < 0.0001$ [CI: -1.336, -0.870]) were significantly upregulated in the UTMD*sv* group compared with those in the OA group. Compared with the US or SV groups, aggrecan ($P < 0.0001$ [CI: -1.285, -0.745]; $P = 0.0013$ [CI: -0.743, -0.205]), collagen II ($P < 0.0001$ [CI: -1.844, -1.204]; $P = 0.0004$ [CI: -1.245, -0.426]) and PPARγ ($P < 0.0001$ [CI: -1.226, -0.759]; $P < 0.0018$ [CI: -0.626, -0.159]) expression levels were significantly increased in the UTMD*sv* group [Fig. 2(A-B)]. Triglyceride absorbance value in chondrocytes was analyzed by oil red O staining [Fig. 2(C-D)]. Compared with the OA group, the

absorbance were significantly decreased ($P = 0.027$; $P = 0.005$; $P < 0.0001$) in the UTMD, SV and UTMD*sv* groups. Compared with the UTMD or SV groups, the absorbancewere significantly reduced ($P = 0.004$ [CI: 0.035, 0.174]; $P = 0.023$ [CI:0.010, 0.149]) in the UTMD*sv* group. To determine if UTMD*sv* affect cholesterol metabolism, we further analyzed cholesterol efflux in each group [Fig. 2E]. Cholesterol efflux was significantly increased ($P = 0.001$; $P < 0.0001$; $P < 0.0001$) compared with that in the OA group. Compared with the UTMD group, the cholesterol efflux level was increased ($P = 0.001$ [CI: -51.63, -27.04]) in the UTMD*sv* group.

The expression level of extracellular matrix proteins after PPARγ inhibitor and UTMDsv intervention

To investigate the involvement of PPARγ in the process of OA cartilage ECM expression and cholesterol efflux rate, we treated chondrocytes with a PPARγ inhibitor (12.5 μM T0070907). Compared with the control group, the expression levels of aggrecan ($P < 0.0001$ [CI:0.222, 0.452]), collagen II ($P < 0.0001$ [CI: 0.451, 0.911]), and PPARγ ($P = 0.0004$ [CI: 0.012, 0.338]) and the cholesterol efflux rate ($P = 0.002$ [CI: 7.531, 25.14]) were significantly decreased in the PPARγ inhibitor group [Fig. 3(A-E)]. Further investigation of the effect of UTMD*sv* on chondrocytes showed that aggrecan ($P = 0.0002$ [CI: -0.391, -0.161]), collagen II ($P < 0.0001$ [CI: -0.711, -0.251]) and PPARγ ($P = 0.0003$ [CI: -0.554, -0.228]) expression levels and the cholesterol efflux rate ($P < 0.0001$ [CI: -34.80, -17.20]) were significantly increased in the UTMD*sv* group compared with those in the PPARγ inhibitor groups [Fig. 3(A-E)].

Pathology score and cholesterol level after UTMDsv intervention

We further investigated the activity of aggrecan, collagen II and PPARγ in vivo after intra-articular injection of UTMD, SV or UTMD*sv*. Safranin-O staining [Fig. 4(A-B)] showed that the Mankin scores were increased ($P < 0.0001$ [CI: -11.94, -5.339]) in the OA group compared with those in the control group. Compared with the SV group, the Mankin scores were decreased ($P = 0.044$ [CI: 0.069, 6.671]) in the UTMD*sv* group. Enzymatic analysis levels of TC and HDL-C levels from synovial fluid showed that the TC level was increased ($P < 0.0001$ [CI: -1.701, -1.051]) in the OA group compared with that in the control group. Compared with the OA group, TC levels were reduced ($P < 0.0001$ [CI: 0.472, 1.122]; $P < 0.0001$ [CI: 0.915, 1.566]) in the SV and UTMD*sv* groups. Compared with the SV group, TC levels were reduced ($P = 0.008$ [CI: 0.118, 0.768]) in the UTMD*sv* group [Fig. 4C]. Compared with the control group, HDL-C was decreased ($P < 0.0001$ [CI: 0.634, 0.910]) in the OA group. Compared with the OA group, HDL-C level were increased ($P < 0.0001$ [CI: -0.592, -0.316]; $P < 0.0001$ [CI: -0.877, -0.600]) in the SV and UTMD*sv* groups. Compared with the SV group, HDL-C was increased ($P = 0.004$ [CI: -0.423, -0.147]) in the UTMD*sv* group [Fig. 4D]. Aggrecan ($P < 0.0001$ [CI: 0.499, 0.827]), collagen II ($P < 0.0001$ [CI: 0.582, 0.875]) and PPARγ ($P < 0.0001$ [CI: 0.288, 0.569]) expression levels were significantly decreased in the OA group compared with those in the control group. Compared with the OA group, aggrecan ($P = 0.000$, [CI: -0.505, -0.177]; $P < 0.0001$ [CI: -0.828, -0.499]), collagen II ($P < 0.0001$ [CI: -0.524, -0.231]; $P < 0.0001$ [CI: -0.823, -0.530]) and PPARγ ($P = 0.0007$ [CI: -0.408, -0.127]; $P < 0.0001$ [CI: -0.652, -0.371]) expression levels were increased in

the SV and UTMD*sv* groups. Compared with the SV group, the expression levels of these proteins were increased ($P = 0.0005$; $P = 0.0004$; $P = 0.0014$) in the UTMD*sv* group [Fig. 4E].

Discussion

In this study, we investigated the ability of UTMD*sv* to regulate the cholesterol efflux rate through PPARγ and delay the degeneration of rabbit OA cartilage. We found that UTMD*sv* increased the expression of PPARγ, aggrecan and collagen II in chondrocytes, promoted the cholesterol efflux rate, and regulated cholesterol metabolism in the joint fluid, thereby delaying the process of OA cartilage degeneration.

Previous studies have reported that aggrecan and collagen II, major ECM proteins, are degraded in the development of OA[24–26]. In the present study, we observed that the expression of aggrecan and collagen II in OA chondrocytes decreased by immunofluorescence staining, indicating that the surface of OA cartilage was damaged. By intervening OA chondrocytes with UTMD*sv*, we found that ECM expression can be activated and subchondral bone pathology reconstruction can be changed to achieve the purpose of cartilage repair.

Superabundant cholesterol in cells can cause toxicity, leading to cell rupture, apoptosis and necrosis[27]. A high cholesterol diet causes cartilage degeneration and the occurrence of OA in a rat experimental model, while reducing cholesterol levels reduced the incidence of cartilage degeneration[28]. The blood circulation is associated to the synovial circulation via the capillaries and lymphatic system. That's probably why we find high cholesterol in joint fluid. Under such circumstances, chondrocytes are exposed to increased cholesterol levels in the synovial fluid, which cause the damage of cartilage ECM protein. If high cholesterol level persisted in the synovia fluid, resulting in chondrocyte hypertrophy and cartilage ossification, which further exacerbates the severity of OA cartilage degeneration[26,29–30]. In our study, we also found that triglycerides were excessively deposited in OA chondrocytes, and the cholesterol efflux rate was decreased.

PPARγ is a key factor in RCT by promoting the cholesterol efflux rate and maintaining the dynamic balance of cholesterol metabolism[31–32]. Studies have shown that PPARγ affects chondrocytes metabolism and lipid metabolism and participates in the occurrence and development of OA. Direct activation of PPARγ can promote cholesterol efflux and reduce lipid deposition in chondrocytes [33]. In our study, we found that the cholesterol efflux rate decreased significantly after inhibiting PPARγ, and the cholesterol efflux rate increased after the PPARγ combined with UTMD*sv* intervention. These findings indicate that PPARγ is a key factor affecting cholesterol efflux, and that UTMD*sv* not only improve the cholesterol efflux rate effectively and also increase the expression of aggrecan and collagen II in chondrocytes.

Simvastatin promoted cholesterol efflux by activating PPARγ[13], reducing lipid deposition- and upregulating the expression of ECM, thus protecting cartilage. Several studies have shown that statins not only reduce blood lipids effectively[34], but also protect against chondrocyte aging and degeneration

and prevent ECM degradation. These functions were shown to protect articular cartilage, reducing the overall rate of knee OA progression by 50%[35–39]. However, a clinical study showed that long-term use of statins can cause myopathy, liver dysfunction, diabetes and cerebral hemorrhage[40–41]. To avoid the adverse reactions caused by oral statins, some studies explored the effect of intra-articular injection of different simvastatin concentrations (0.01 mg/mL, 0.1 mg /mL, and 0.5 mg/mL) on early OA cartilage degeneration in rabbits. The results showed that 0.5 mg/mL simvastatin has a significantly protective effect on early rabbit OA [42]. In this study, injection of 0.1 mg/mL simvastatin microbubbles into the joint cavity of OA rabbits significantly reduced the Mankin score, while the expression levels of aggrecan, collagen II, and PPARγ were significantly increased.

UTMD can cause the continuous compression and expansion that induces microbubble rupture, which can improve the efficacy of drugs and reduce the dosage[43–44]. Studies have shown that microbubbles can improve the delivery of drugs and reduce the adverse effects caused in the gastrointestinal tract by oral administration[45]. In addition, UTMD can reduce the required intensity and duration of US and avoid the detrimental effects of US cavitation, such as damage to cell membranes, breakage of DNA chains, inhibition of cell proliferation, promotion of apoptosis and other adverse reactions[46]. Some in vitro studies have indicated that US can induce the oxidative stress response of cell membrane lipids by interfering with lactobacillus cells, thereby promoting cholesterol efflux[47]. However, in our study, US alone did not significantly increase the cholesterol efflux rate or reduce TC levels, although we found that low-intensity US combined with statin microbubbles affected cholesterol efflux. We also found that UTMD*sv* significantly reduced cholesterol efflux and increased the expression of collagen II and aggrecans.

In summary, our results verified that UTMD*sv* can promote rabbit knee OA cartilage ECM expression both in vivo and in vitro. The main mechanism may be related to PPARγ-mediated regulation of lipid metabolism, promotion of cholesterol efflux, and elimination of chondrocyte lipids.

Abbreviations

OA: osteoarthritis; PPARγ: peroxisome proliferator-activated receptor; TC: total cholesterol; HDL-C: high-density lipoprotein-cholesterol; US: ultrasound; SV: simvastatin; UTMD: ultrasound-targeted microbubble destruction; UTMD$_{SV}$: ultrasound-targeted simvastatin-loaded microbubble destruction; WB: western blotting; ACLT: anterior cruciate ligament transection; DMEM: Dulbecco's modified Eagle's medium; FBS: fetal bovine serum; DAPI: diamidino phenylindole; DPPC: dipalmitoyl phosphatidyl choline; PVDF: polyvinylidene fluoride; TBST: Tween-Tris buffered saline; GAPDH: glyceraldehyde-3-phosphate dehydrogenase; RPMI: Roswell Park Memorial Institute.

Declarations

Acknowledgments

We thank the National Natural Science Foundation of China (No. 81772437, 82072541) for financial support.

Funding

This work was supported by the National Natural Science Foundation of China (Grant Number 81772437, 82072541).

Availability of data and materials

All data generated and/or analyzed during this study are included in this published article.

Author Contributions

PX and XL conceived and designed the study. XW and DW performed the experiments. XW wrote the manuscript. XW, QW and JS collected and analyzed data. KC and QL reviewed and edited the manuscript. All authors read and approved the manuscript.

Ethics approval and consent to participate

The experimental protocol relating to rabbits was approved by the Nanjing Medical University Ethics Committee of Nanjing Hospital (20150829).

Competing interests

The authors declare that they have no competing interests.

References

1. Neogi T, Zhang Y. Epidemiology of osteoarthritis[J]. Rheum Dis Clin North Am, 2013,39(1):1-19.
2. Conaghan P G, Kloppenburg M, Schett G, Bijlsma JW. Osteoarthritis research priorities: a report from a EULAR ad hoc expert committee[J]. Ann Rheum Dis, 2014,73(8):1442-1445.
3. Wang X, Hunter D, Xu J, Ding C. Metabolic triggered inflammation in osteoarthritis[J]. Osteoarthritis Cartilage, 2015,23(1):22-30.
4. Si H B, Zeng Y, Liu S Y, Zhou ZK, Chen YN, Cheng JQ, et al. Intra-articular injection of microRNA-140 (miRNA-140) alleviates osteoarthritis (OA) progression by modulating extracellular matrix(ECM) homeostasis in rats[J]. Osteoarthritis Cartilage, 2017,25(10):1698-1707.
5. Chawla A, Boisvert W A, Lee C H, Laffitte BA, Barak Y, Joseph SB, et al. A PPAR gamma-LXR-ABCA1 pathway in macrophages is involved in cholesterol efflux and atherogenesis[J]. Mol Cell, 2001,7(1):161-171.
6. Kostopoulou F, Malizos K N, Papathanasiou I, Tsezou A. MicroRNA-33a regulates cholesterol synthesis and cholesterol efflux-related genes in osteoarthritic chondrocytes[J]. Arthritis Res Ther, 2015,17:42.

7. Masuko K, Murata M, Suematsu N, Okamoto K, Yudoh K, Nakamura H, et al. A metabolic aspect of osteoarthritis: lipid as a possible contributor to the pathogenesis of cartilage degradation[J]. Clin Exp Rheumatol, 2009,27(2):347-353.
8. Tosheska Trajkovska K, Topuzovska S. High-density lipoprotein metabolism and reverse cholesterol transport: strategies for raising HDL cholesterol[J]. Anatol J Cardiol, 2017,18(2):149-154.
9. Faezeh Vasheghani, Meryem Blati, Hassan Fahmi, Yue Zhang, Ying-hua Li, Bertrand Lussier, et al. PPARγ deficiency results in severe, accelerated osteoarthritis associated with aberrant mTOR signalling in the articular cartilage[J]. Basic and translational research,2015,8(2):
10. Jiang T, Ren K, Chen Q, Li H, Yao R, Hu H, et al. Leonurine Prevents Atherosclerosis Via Promoting the Expression of ABCA1 and ABCG1 in a PPARγ/Lxrα Signaling Pathway-Dependent Manner[J]. Cellular Physiology and Biochemistry, 2017, 43(4): 1703-1717.
11. Tsezou A, Iliopoulos D, Malizos K N, Simopoulou, T. Impaired expression of genes regulating cholesterol efflux in human osteoarthritic chondrocytes[J]. Journal of Orthopaedic Research, 2010, 28(8): 1033-1039.
12. Chang C H, Hsu Y M, Chen Y C, Lin F H, Subramaniam S, Siowtung L, et al. Anti-inflammatory effects of hydrophilic and lipophilic statins with hyaluronic acid against LPS-indu ced inflammation in porcine articular chondrocytes[J]. J Orthop Res, 2014,32(4):557-565.
13. Tenenbaum A, Fisman E Z. Balanced pan-PPAR activator bezafibrate in combination with statin: comprehensive lipids control and diabetes prevention?[J]. Cardiovasc Diabetol, 2012,11:140.
14. Bayyurt S, Kü Ükalp A, Bilgen M S, Bilgen, ÖF, Çavuşoğlu, İ, Yalçınkaya, U. The chondroprotective effects of intraarticular application of statin in osteoarthritis: An experimen tal study[J]. Indian J Orthop, 2015,49(6):665-671.
15. Park D, Ryu H, Kim H S, Kim Y, Choi K, Park H, et al. Sonophoresis Using Ultrasound Contrast Agents for Transdermal Drug Delivery: An In Vivo Experimental Study[J]. Ultrasound in Medicine & Biology, 2012, 38(4):642-650.
16. Zahra Izadifar, Paul Babyn, Dean Chapman. Ultrasound Cavitation/Microbubble Detection and Medical Applications[J]. Journal of Medical and Biological Engineering,2019,39(3).
17. Liao A, Chung H, Chen W, Yeh M. Efficacy of Combined Ultrasound-and-Microbubbles- Mediated Diclofenac Gel Delivery to Enhance Transdermal Permeation in Adjuvant-Induced Rheumatoid Arthritis in the Rat[J]. Ultrasound in Medicine & Biology, 2016, 42(8):1976-1985.
18. Liao A H, Chuang H C, Chung H Y. Efficacy of ultrasound mediated microbubbles in diclofenac gel to enhance transdermal permeation in rheumatoid arthritis induced rat[J]. Conf Proc IEEE Eng Med Biol Soc, 2015, 2015(8):3521-3524.
19. Jean Y H, Wen Z H, Chang Y C, Hsieh SP, Lin JD, Tang CC, et al. Increase in excitatory amino acid concentration and transporters expression in osteoarthritic knees of anterior cruciate ligament transected rabbits[J]. Osteoarthritis Cartilage, 2008,16(12):1442-1449.
20. Sheng P, Zhu H, Zhang W, Xu Y, Peng W, Sun J, et al. The immunoglobulin superfamily member 3 (IGSF3) promotes hepatocellular carcinoma progression through activation of the NF-κB pathway[J].

Ann Transl Med, 2020, 8(6):378-391.

21. An Z, Yu JR, Park WY. T0070907 inhibits repair of radiation-induced DNA damage by targeting RAD51[J]. Toxicol In Vitro, 2016,12(37):1-8
22. Singla R, Soni S, Padwad YS, Acharya A, Yadav SK . Sustained delivery of BSA/HSA from biocompatible plant cellulose nanocrystals for in vitro cholesterol release from endothelial cells[J]. International journal of biological macromolecules,2017,104(Pt A): 748-757
23. Wang XJ, Zhang ZH, Zhang J, Yu JP, An XJ, Zhou XS, et al. Malfunction of autophagy in tibial growth plate chondrocytes causes increased apoptosis rate in chronic renal insufficiency rats[J]. Zhonghua Yi Xue Za Zhi,2020,100(2):141-145
24. Pun YL, Moskowitz RW,Lie S, Sundstrom WR, Block SR, McEwen C, et al. Clinical correlations of osteoarthritis associated with a single-base mutation (arginine519 to cysteine) in type ii procollagen gene[J]. Arthritis & Rheumatism,1994, 37(2):264-269
25. Tanaka N□TashiroT, Katsuragawa Y, Sawabe M, Furukawa H, Fukui N. Expression of minor cartilage collagens and small leucine rich aggrecans may be relatively reduced in osteoarthritic cartilage[J]. BMC Musculoskelet Disor□2019□20(1):232-242
26. Zhu G, Qian Y, Wu W, Li R. Negative effects of high mechanical tensile strain stimulation on chondrocyte injury in vitro[J]. Biochem Biophys Res Commun, 2019, 510(1):48-52
27. Litvinov D Y, Savushkin E V, Garaeva E A, Dergunov AD. Cholesterol Efflux and Reverse Cholesterol Transport: Experimental Approaches[J]. Curr Med Chem, 2016,23(34):3883-3908.
28. Gierman L M, Der Ham F V, Koudijs A, Wielinga PY, Kleemann R, Kooistra T, et al. Metabolic Stress–Induced Inflammation Plays a Major Role in the Development of Osteoarthritis in Mice[J]. Arthritis Rheum, 2012, 64(4): 1172-1181.
29. Ajay Chawla, William A B, Chih-Hao Lee, Yaacov Barak, Debbie Liao, Ronald M E, et al. A PPARg-LXR-ABCA1 Pathway in Macrophages Is Involved in Cholesterol Efflux and Atherogenesis[J]. Molecular Cell, 2001,7:161-171.
30. Fahmi H, Martel-Pelletier J, Pelletier JP, Kapoor M. Peroxisome proliferator-activated receptor gamma in osteoarthritis[J]. Mod Rheumatol, 2011, 21(1):1-9.
31. Wang M D, Franklin V, Marcel Y L. In vivo reverse cholesterol transport from macrophages lacking ABCA1 expression is impaired[J]. Arterioscler Thromb Vasc Biol, 2007,27(8):1837-1842.
32. Vedhachalam C, Liu L, Nickel M, Dhanasekaran P, Anantharamaiah GM, Lund-Katz S, et al. Influence of ApoA-I structure on the ABCA1-mediated efflux of cellular lipids[J]. J Biol Chem, 2004,279(48):49931-49939.
33. Zhu X, Chen F, Lu K, Wei A, Jiang Q, Cao W . PPARγ preservation via promoter demethylation alleviates osteoarthritis in mice[J]. Ann Rheum Dis, 2019, 78(10):1420-1429.
34. Adams SP, Alaeiilkhchi N, Wright JM. Pitavastatin for lowering lipids[J]. Cochrane Database Syst Rev, 2020, 6:CD012735.

35. Simopoulou T, Malizos K N, Poultsides L, Tsezou A. Protective effect of atorvastatin in cultured osteoarthritic chondrocytes.[J]. Journal of Orthopaedic Research, 2009, 28(1): 110-115.
36. Bayyurt S, Kucukalp A, Bilgen M S, Bilgen ÖF, Çavuşoğlu İ, Yalçınkaya U . The chondroprotective effects of intraarticular application of statin in osteoarthritis: An experimental study[J]. Indian Journal of Orthopaedics, 2015, 49(6): 665-671.
37. Dinc M, Bilgen M S, Kucukalp A, Bilgen OF. An Assessment of the Chondroprotective Effects of Intra-Articular Application of Statin and Tetracycline on Early-Stage Experimental Osteoarthritis[J]. International Scholarly Research Notices, 2012: 182097-182097.
38. Conaghan P G. The effects of statins on osteoarthritis structural progression: another glimpse of the Holy Grail?[J]. Annals of the Rheumatic Diseases, 2012, 71(5): 633-634.
39. Yudoh K , Karasawa R . Statin prevents chondrocyte aging and degeneration of articular cartilage in osteoarthritis (OA).[J]. Aging, 2010, 2(12):990-998.
40. Collins R, Reith C, Emberson J, Armitage J, Baigent C, Blackwell L, et al. Interpretation of the evidence for the efficacy and safety of statin theray[J]. Lancet, 2016,388(10059):2532-2561.
41. K Siddiqui M, Maroteau C, Veluchamy A, Tornio A, Tavendale R, Carr F, et al. A common missense variant of LILRB5 is associated with statin intolerance and myalgia[J]. Eur Heart, 2017,38(48):3569-3575.
42. Fan Li. Experimental study of simvastatin in preventing and treating osteoarthritis[J]. Huazhong University of Science and Technology, 2010.
43. Liang H, Tang J, Halliwell M. Sonoporation, drug delivery, and gene therapy. Proceedings of the Institution of Mechanical Engineers[J]. Journal of Engineering in Medicine, 2010224(2), 343–361.
44. Dijkmans PA, Jufermans LJM, Musters RJP, van Wamel A, ten Cate FJ, van Gilst W, et al. Microbubbles and ultrasound: from diagnosis to therapy[J]. Echocardiogr,2004,5(4):245–256.
45. Liu F, Zhu J, Huang Y, Guo W, Rui M, Xu Y, et al. Hypolipidemic effect of SR?BI gene delivery by combining cationic liposomal microbubbles and ultrasound in hypercholesterolemic rats[J]. Mol Med Rep, 2013,7(6):1965-1969.
46. Lu QL, Liang H D, Partridge T, Blomley MJK. Microbubble ultrasound improves the efficiency of gene transduction in skeletal muscle in vivo with r educed tissue damage[J]. Gene Ther,2003,10(5):396-405.
47. Lye H S, Alias K A, Rusul G, Liong MT. Ultrasound treatment enhances cholesterol removal ability of lactobacilli[J]. Ultrason Sonochem, 2012,19(3):632-641.

Figures

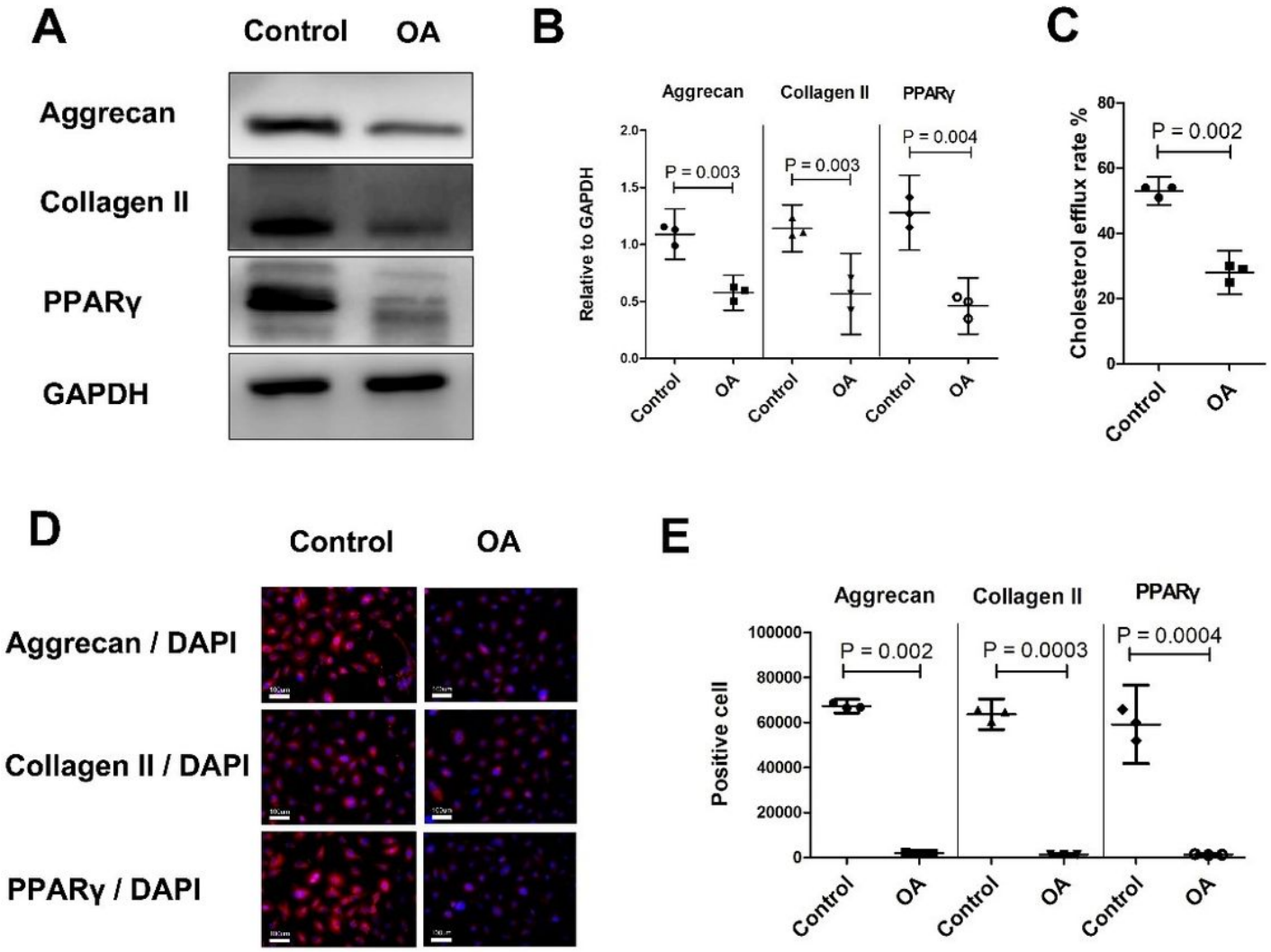

Figure 1

The ECM expression and cholesterol efflux rate decreases in OA chondrocytes. (A-B) WB analysis of aggrecan, collagen II and PPARγ expression in chondrocytes. GAPDH was used as endogenous genes. (C) The difference in cholesterol efflux rate between the control and OA groups; (D-E) Representative immunofluorescence staining and quantification of the positive cells number. Chondrocytes are stained blue and the target proteins are stained red(scale bar=100 μm).

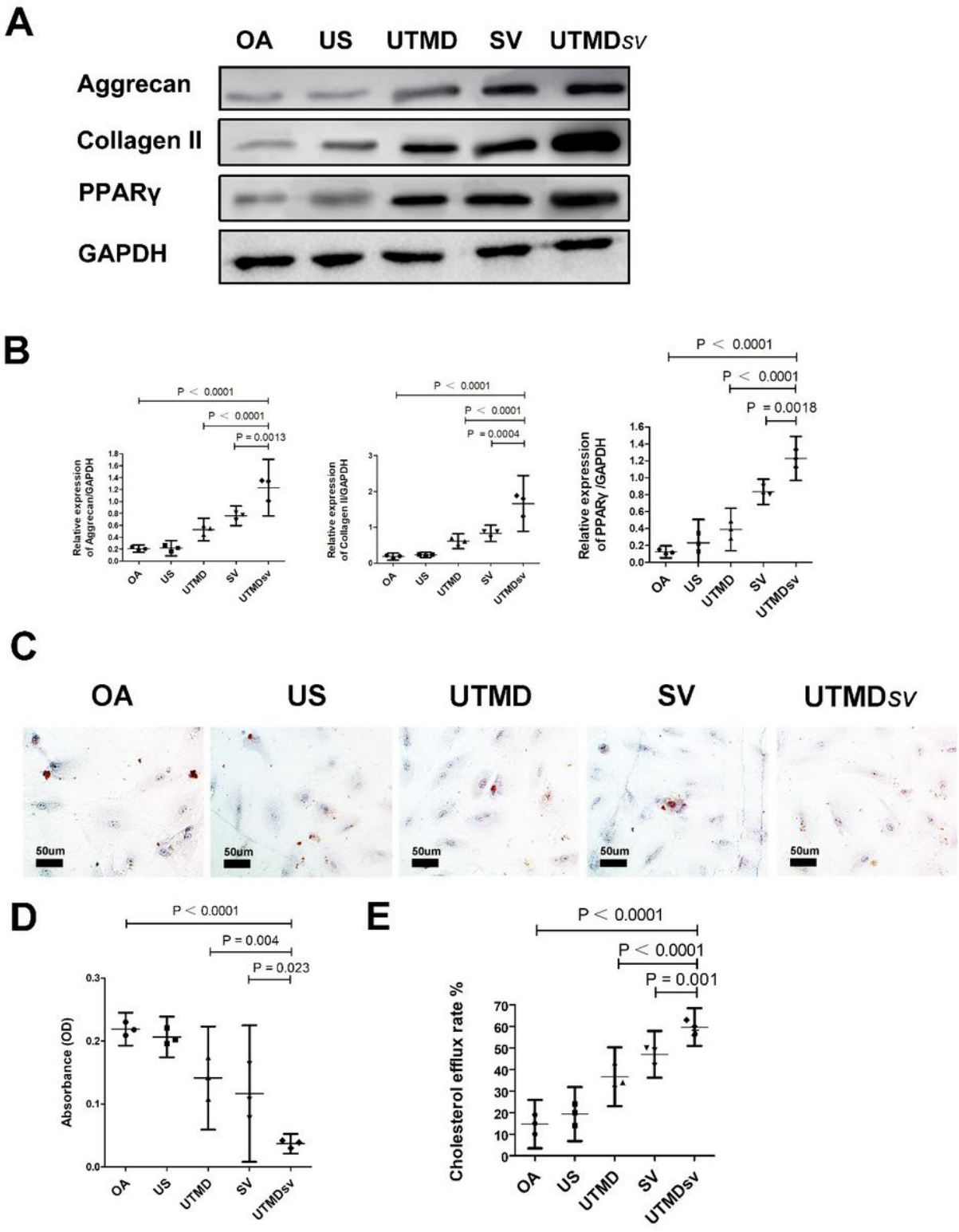

Figure 2

Effects of UTMDsv on cartilage metabolism and lipid metabolism. (A-B) Representative WB and quantification of aggrecan, collagen II, PPARγ and GAPDH expression in OA chondrocytes after treatment with US, UTMD, SV and UTMDsv. (C) Representative oil red images; scale bar=50 μm. (D) Triglyceride levels was quantified in chondrocytes by measuring absorbance at 490 nm. (E) The difference in cholesterol efflux rate between groups.

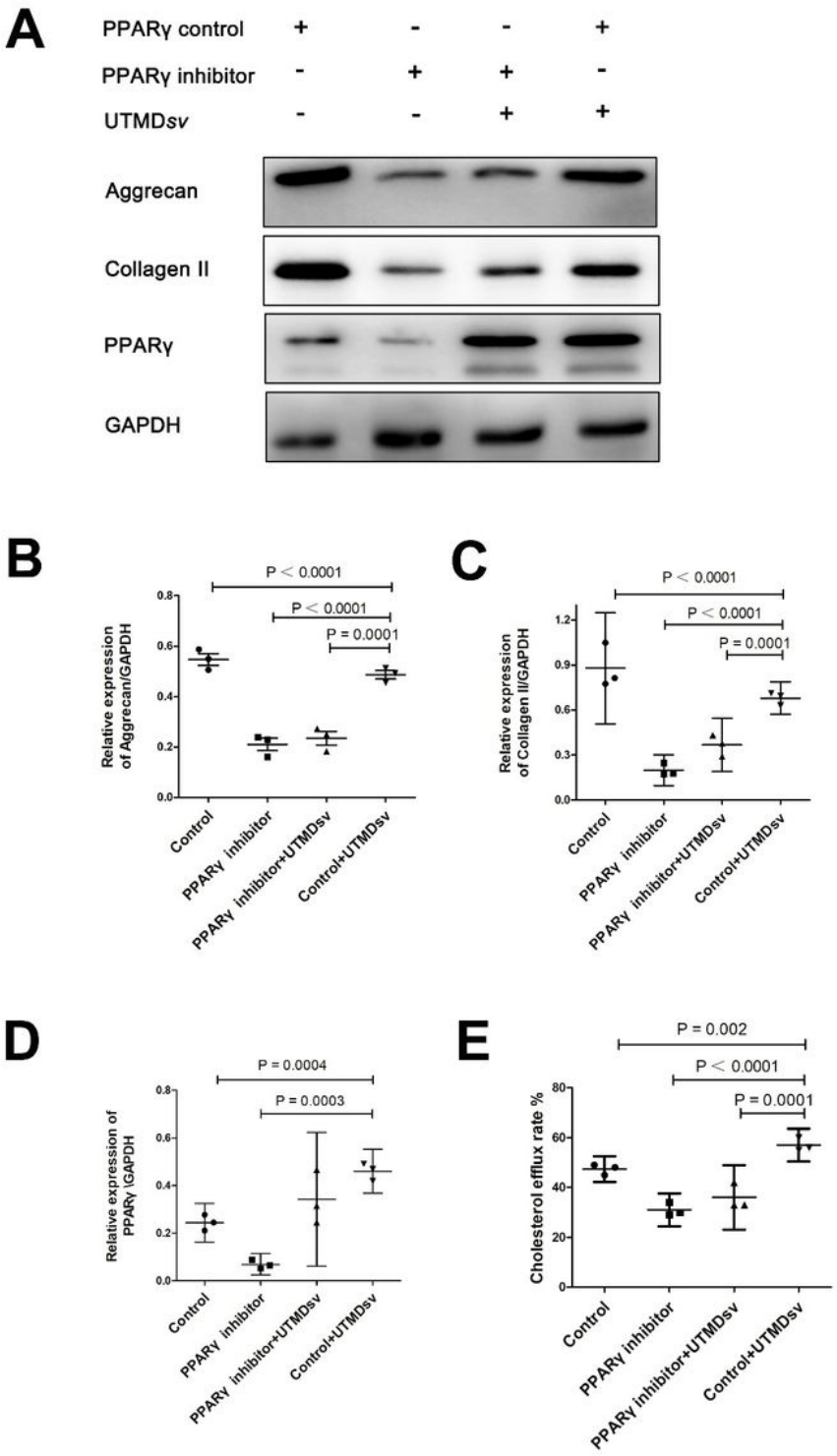

Figure 3

PPARγ inhibitor reduces the ECM expression and the cholesterol efflux rate in chondrocyte. The chondrocytes were treated with PPARγ inhibitor. (A-D) WB and quantitation of the relative expression levels of aggrecan, collagen II and PPARγ after PPARγ inhibitor and UTMDsv intervention in OA chondrocytes; GADPH was used as endogenous protein. (E) The effect of the PPARγ inhibitor and UTMDsv on the cholesterol efflux rate.

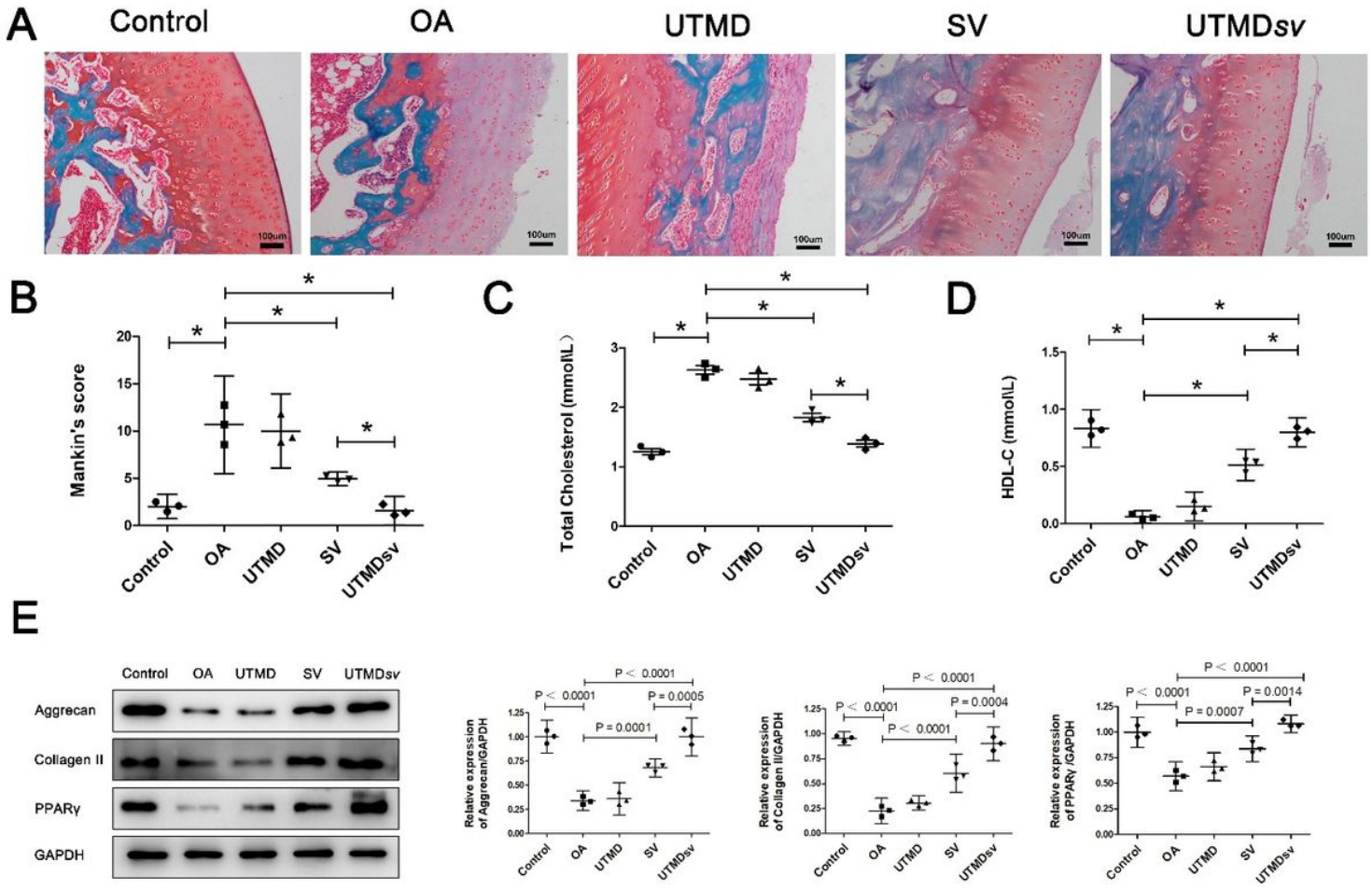

Figure 4

Effects of UTMDsv on cholesterol regulation and cartilage metabolism in OA rabbit. Animals were respectively treated with UTMD, SV and UTMDSV every 7 days for 4 weeks. Equivalent saline was administered into the control and OA groups. (A-B) The representative safranin-O images and Mankin scoring of OA parameters(n=3). (C-D) The levels of TC and HDL-C in rabbit knee synovial fluid were detected by enzyme-marker assay. (E) WB and quantitation of the relative expression levels of aggrecan, collagen II, PPARγ and GADPH(n=3).

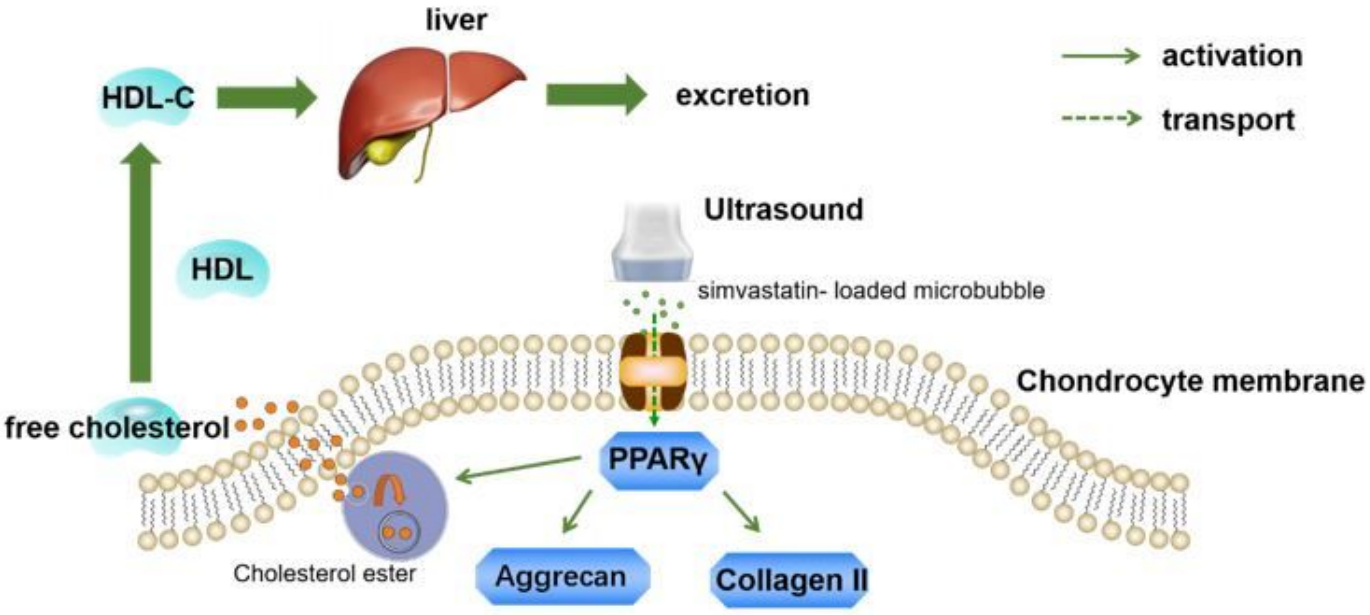

Figure 5

Simplified scheme of cholesterol efflux pathway mediated by PPARγ in chondrocytes.